The Astrophysical Journal, 668:81–86, 2007 October 10

SWIFT XRT OBSERVATION OF 34 NEW *INTEGRAL* IBIS AGNs: DISCOVERY OF COMPTON-THICK AND OTHER PECULIAR SOURCES

A. Malizia,[1] R. Landi,[1] L. Bassani,[1] A. J. Bird,[2] M. Molina,[2] A. De Rosa,[3] M. Fiocchi,[3] N. Gehrels,[4] J. Kennea,[5] and M. Perri[6]

Received 2007 April 17; accepted 2007 June 12

ABSTRACT

For a significant number of the sources detected at high energies (>10 keV) by the *INTEGRAL* IBIS and *Swift* BAT instruments there is either a lack information about them in the 2–10 keV range or they are totally unidentified. Herein, we report on a sample of 34 IBIS AGNs or AGN candidate objects for which there is X-ray data in the *Swift* XRT archive. Thanks to these X-ray follow-up observations, the identification of the gamma-ray emitters has been possible and the spectral shape in terms of photon index and absorption has been evaluated for the first time for the majority of our sample sources. The sample, enlarged to include four more AGNs already discussed in the literature, has been used to provide photon index and column density distribution. We obtain a mean value of 1.88 with a dispersion of 0.12, i.e., typical of an AGN sample. Sixteen objects (47%) have column densities in excess of 10^{22} cm^{-2} and, as expected, a large fraction of the absorbed sources are within the Sey 2 sample. We have provided a new diagnostic tool ($N_{\rm H}$ vs. $F_{2-10\,\rm keV}/F_{20-100\,\rm keV}$ softness ratio) to isolate peculiar objects; we find at least one absorbed Sey 1 galaxy, three Compton-thick AGN candidates; and one secure example of a "true" type 2 AGN. Within the sample of 10 still unidentified objects, 3 are almost certainly AGNs of type 2; 3–4 have spectral slopes typical of AGN; and 2 are located high on the Galactic plane and are strong enough radio emitters that they can be considered good AGN candidates.

Subject headings: galaxies: Seyfert — X-rays: general

Online material: color figure

1. INTRODUCTION

In the last few years, our knowledge of the hard X-ray sky (>10 keV) has improved greatly thanks to the observations made by IBIS (Ubertini et al. 2003) on board *INTEGRAL* (Winkler et al. 2003) and BAT (Barthelmy et al. 2005) on board *Swift* (Gehrels et al. 2004); both telescopes operate in similar wave bands (around 20–200 keV) with a sensitivity of about a millicrab and a point-source location accuracy of the order of a few arcminutes. These instruments have so far been used to survey the high-energy sky in a complementary way, as the first concentrates mainly on mapping the Galactic plane, while the second mainly covers the high Galactic latitude sky, so that together they will provide the best yet sample of objects selected in the soft gamma-ray band. For a significant number of the sources detected by these two satellites there is either a lack of information about them in the 2–10 keV range or they are totally unidentified. For example, the third *INTEGRAL* IBIS survey (Bird et al. 2007) contains 421 hard X-ray (17–100 keV) emitters of which 113 are unidentified objects (26% of the entire sample); around 140 sources are AGNs or AGN candidates and for almost half of these there is no information below 10 keV. For all these objects, improved localization, as is now possible with the current generation of focusing X-ray telescopes, is necessary in order to pinpoint the optical counterpart and to definitely resolve their nature/class. Spectral information in the X-ray band is equally necessary in order to characterize the source spectral shape. For these reasons, a program of X-ray follow-up observations of *INTEGRAL* IBIS sources has recently been initiated with the *Swift* satellite using the XRT instrument (0.2–10 keV; Burrows et al. 2005). Herein we report on a sample of 34 AGNs or AGN candidates for which there is X-ray data in the *Swift* XRT archive up to the end of 2007 February. For the majority of these sources the X-ray spectra are presented for the first time. Previously, for a third of the sample only an estimate of the column densities have been reported by Sazonov et al. (2007); our results are in good agreement with theirs. XRT follow-up measurements allow, in all cases, an arcsecond positioning of the X-ray counterpart and in most objects a definition of the X-ray spectral shape, in terms of photon index and column density estimates. In particular, the study of the column density distribution in a sample of AGNs selected above 10 keV is important, so as to quantify the fraction of objects missed by lower energy surveys, to find new Compton-thick AGNs or peculiar sources, and as an input parameter for synthesis models of the cosmic X-ray background. All our sources have redshifts $z < 0.08$, and so our results refer to the local universe.

2. *Swift* XRT IMAGE ANALYSIS

Due to the pointing strategy of *Swift*, short (a few ks) repeated (up to 5 times) measurements are typically performed for each target. Table 1 lists for each *INTEGRAL* IBIS source, the XRT position and the 90% error box of the X-ray counterpart, the number of pointings,[7] the total exposure time available, the mean count rates (i.e., related to the sum of all available observations) of the detected X-ray counterpart in the best energy range (see § 3), and, finally, its class and redshift (from the NASA/IPAC Extragalactic Database [NED], unless otherwise stated).

[1] IASF-Bologna/INAF, via P. Gobetti 101, 40129 Bologna, Italy.
[2] School of Physics and Astronomy, University of Southampton, Highfield, Southampton, SO17 1BJ, UK.
[3] IASF-Roma/INAF, via del Fosso del Cavaliere 100, 00133 Roma, Italy.
[4] NASA/Goddard Space Flight Center, Greenbelt, MD 20771.
[5] Department of Astronomy and Astrophysics, Pennsylvania State University, University Park, PA 16802.
[6] ASI Science Data Center, via G. Galilei, 00044 Frascati, Italy.

[7] In a few cases some observations have not been considered due to their poor quality and/or short duration (<1 ks).

TABLE 1
Swift XRT Positions

Source	R.A.	Decl.	Error (arcsec)	No. of Observations	Exposure Time (s)	Count Rate (counts s^{-1})	Class	Class Ref.	Redshift
IGR J02097+5222	02 09 37.68	+52 26 43.56	3.54	2	8034	0.366±0.0067	Sey 1		0.049
SWIFT J0216.3+5128	02 16 27.01	+51 25 25.50	3.56	3	16401	0.169±0.0032	??		...
NGC 1142	02 55 12.19	−00 11 02.31	3.80	4	18807	0.034±0.0013	Sey 2		0.029
1H 0323+342	03 24 41.04	+34 10 45.49	3.53	3	19510	0.368±0.0043	Sey 1		0.061
LEDA 168563	04 52 04.85	+49 32 43.72	3.59	1	1111	0.297±0.0016	Sey 1		0.029
IGR J07565−4139	07 56 19.71	−41 37 41.62	3.75	1	14750	0.020±0.0012	Sey 2	1	0.021
IGR J07597−3842	07 59 41.66	−38 43 57.35	3.52	4	19753	0.383±0.0044	Sey 1.2	1	0.040
SWIFT J0917.2−6221	09 16 09.01	−62 19 29.04	3.56	2	12893	0.202±0.0039	Sey 1		0.057
IGR J10404−4625	10 40 22.27	−46 25 24.69	3.61	4	19561	0.064±0.0018	Sey 2	2	0.024
IGR J12391−1612	12 39 05.98	−16 10 48.14	3.62	1	6625	0.106±0.0046	Sey 2		0.037
IGR J12415−5750	12 41 25.36	−57 50 03.97	3.57	2	12843	0.137±0.0033	Sey 2		0.024
ESO 323-G077	13 06 26.13	−40 24 53.22	3.72	2	7953	0.018±0.0015	Sey 1.2		0.015
IGR J13109−5552	13 10 43.08	−55 52 11.66	3.73	2	6563	0.092±0.0037	??		...
IGR J14003−6326	14 00 45.35	−63 25 41.17	3.77	2	5010	0.174±0.0071	??		...
IGR J14175−4641	14 17 03.94	−46 41 39.06	5.70	1	5541	0.009±0.0007	Sey 2	1	0.076
IGR J14471−6319	14 47 14.69	−63 17 19.56	4.03	1	3911	0.033±0.0029	Sey 2	1	0.038
IGR J14492−5535	14 49 12.67	−55 36 20.32	3.77	1	3606	0.016±0.0022	??		...
IGR J14515−5542	14 51 33.43	−55 40 39.41	3.60	3	12515	0.096±0.0028	Sey 2	1	0.018
IGR J14552−5133	14 55 17.36	−51 34 15.68	3.61	2	8423	0.216±0.0051	NLSey1	1	0.016
IGR J15539−6142	15 53 35.22	−61 40 55.40	4.71	1	4840	0.006±0.0013	??		0.015
IGR J16351−5806	16 35 13.42	−58 04 49.69	5.08	2	6233	0.006±0.0009	Sey 2		0.009
IGR J16482−3036	16 48 14.94	−30 35 06.06	3.54	1	9205	0.209±0.0048	Sey 1		0.031
IGR J16558−5203	16 56 05.73	−52 03 41.18	3.52	1	12850	0.438±0.0060	Sey 1.2	1	0.054
SWIFT J1656.3−3302	16 56 16.83	−33 02 12.18	3.73	2	9152	0.071±0.0028	??		...
IGR J17488−3253	17 48 54.82	−32 54 47.83	3.53	1	16780	0.196±0.0035	Sey 1	1	0.020
IGR J18244−5622	18 24 19.49	−56 22 08.72	4.39	1	1631	0.047±0.0054	Sey 2	1	0.017
IGR J18259−0706	18 25 57.25	−07 10 24.54	3.71	1	4260	0.055±0.0036	??		...
IGR J19443+2117	19 43 56.20	+21 18 22.95	3.53	1	11080	0.267±0.0049	??		...
IGR J20186+4043	20 18 38.46	+40 40 59.16	4.81	1	2439	0.008±0.0019	??		...
IGR J20286+2544	20 28 35.05	+25 44 01.57	4.61	1	45385	0.012±0.0016	Sey 2	3	0.014
IGR J21178+5139	21 17 47.24	+51 38 53.62	10.0	2	5362	0.016±0.0018	??		...
IGR J21247+5058	21 24 39.44	+50 58 24.41	3.52	2	10190	0.428±0.0065	Sey 1		0.020
SWIFT J2127.4+5654	21 27 45.58	+56 56 35.64	3.53	2	10130	0.374±0.0061	NLSey1	4	0.014
NGC 7603	23 18 56.69	+00 14 38.22	3.51	3	22860	0.494±0.0047	Sey 1.5		0.029

Note.—Units of right ascension are hours, minutes, and seconds, and units of declination are degrees, arcminutes, and arcseconds.
References.—(1) Masetti et al. 2006c; (2) Masetti et al. 2006a; (3) Masetti et al. 2006b; (4) Halpern 2006.

XRT data reduction was performed using the XRTDAS version 2.0.1 standard data pipeline package (XRTPIPELINE ver. 0.10.6), in order to produce screened event files. All data are extracted only in the photon counting (PC) mode (Hill et al. 2004), adopting the standard grade filtering (0–12 for PC) according to the XRT nomenclature. Images have been extracted in the 0.3–10 keV band and searched for significant excesses falling within the *INTEGRAL* IBIS 90% confidence circle as reported in Bird et al. (2007); in all cases, a single X-ray source was detected either inside this uncertainty circle or just at its border. All sources are detected above 3 σ significance level and in most cases are quite bright at X-ray energies, so that even a short exposure can provide useful information.

The overall sample consists of 11 Seyferts of type 2 (Sey 2) and 13 Seyferts of type 1 (Sey 1; i.e., type in the range 1–1.5), including two narrow-line Seyfert 1s. Ten sources are still optically unclassified and their extragalactic nature is inferred by indirect arguments. Three objects (IGR J14492−5535, IGR J15539−6142, and IGR J20186+4043) are associated with galaxies (2MASX J14491283−5536194, ESO 136-G006, and 2MASX J20183871+4041003, respectively) in which the nuclear activity was unknown before X-/gamma-ray measurements; their AGN class is still uncertain, but the presence of strong absorption in the X-ray spectra implies a type 2 nature (see also § 3). Three other objects (SWIFT J0216.3+5128, IGR J13109−5552, and SWIFT J16563−3302) are located 6° above the Galactic plane and are all radio-emitting objects, besides being strong high-energy emitters; in particular, IGR J13109−5552 and SWIFT J16563−3302, associated with PMN J1310−5552 and NVSS J165616−330211, respectively, are quite strong at radio frequencies (353 mJy at 4.85 MHz for the former and 410 mJy at 20 cm for the latter). Historically, AGNs were discovered by radio observations, i.e., radio selection is often a way in which to recognize active galaxies, except at lower luminosities where also starburst galaxies emit at radio frequencies. Therefore, for bright objects located away from the Galactic plane, mere detection in radio provides support for the presence of an active nucleus. Contamination from Galactic sources may come from pulsars, microquasars, and supernova remnants (Molina 2004), so that it is less easy to claim an AGN association for radio objects on the Galactic plane such as IGR J14003−6362, IGR J18259−0706, IGR J19443+2117, and IGR J21178+5139. However, IGR J19443+2117 is a flat spectrum radio source, according to NED, while IGR J21178+5139 is also a Two Micron All Sky Survey (2MASS) extended object, although not recognized as a galaxy (which is the usual association in this catalog). Clearly, all these sources must await optical (or even

TABLE 2
Swift XRT Spectra

Source	Band (keV)	N_{HGal} ($\times10^{21}$ cm^{-2})	Γ	N_H ($\times10^{22}$ cm^{-2})	$F_{2-10\,keV}$[a] ($\times10^{-11}$ erg cm^{-2} s^{-1})	χ^2/dof	$F_{20-100\,keV}$[a] ($\times10^{-11}$ erg cm^{-2} s^{-1})
IGR J02097+5222	0.5–7.0	1.69	$1.88^{+0.06}_{-0.06}$	...	1.30	107.5/129	2.90
SWIFT J0216.3+5128	1.0–8.0	1.58	$1.91^{+0.13}_{-0.13}$	$1.27^{+0.16}_{-0.14}$	1.27	106.9/117	3.79
NGC 1142	1.0–7.0	0.64	1.8 (fixed)	$44.9^{+4.3}_{-4.0}$	0.96	33.7/26	5.33
1H 0323+342	0.2–7.0	1.44	$2.13^{+0.03}_{-0.04}$	...	0.94	179.7/185	4.21
LEDA 168563	0.8–7.0	5.42	$2.06^{+0.18}_{-0.17}$	...	4.54	10.2/16	6.31
IGR J07565−4139	1.0–6.0	4.73	$1.73^{+0.43}_{-0.47}$	$0.59^{+0.45}_{-0.42}$	0.15	27.6/27	1.78
IGR J07597−3842[b]	1.0–7.2	6.04	$1.80^{+0.04}_{-0.04}$	...	2.37	241.5/259	3.89
SWIFT J0917.2−6221	1.0–7.0	1.91	$1.57^{+0.16}_{-0.14}$	$0.47^{+0.15}_{-0.13}$	1.44	180.1/121	2.20
IGR J10404−4625[b]	1.0–7.0	1.36	$1.47^{+0.30}_{-0.27}$	$2.67^{+0.65}_{-0.54}$	0.72	90.0/80	3.27
IGR J12391−1612	1.0–8.5	0.37	$1.72^{+0.36}_{-0.32}$	$3.08^{+0.84}_{-0.67}$	1.11	33.7/43	6.26
IGR J12415−5750	1.0–6.0	3.45	$1.63^{+0.08}_{-0.07}$	...	0.77	69.6/79	2.32
ESO 323-G077[b,c]	0.5–6.0	0.70	$2.40^{+0.44}_{-0.44}$	$6.61^{+1.24}_{-1.18}$	1.03	41.5/50	2.94
IGR J13109−5552	0.5–7.0	2.76	$1.50^{+0.12}_{-0.12}$	...	0.51	40.9/54	2.46
IGR J14003−6326	1.0–6.0	15.0	$2.21^{+0.39}_{-0.38}$	$1.28^{+0.64}_{-0.62}$	1.43	34.3/40	1.51
IGR J14175−4641[d]	...	...	...	...	0.006	...	1.41
IGR J14471−6319	1.0–7.0	58.0	$1.70^{+1.04}_{-1.03}$	$2.44^{+2.06}_{-1.76}$	0.39	5.8/10	1.47
IGR J14492−5535	2.0–8.5	4.99	1.8 (fixed)	$9.3^{+6.0}_{-4.8}$	0.42	19.0/24	1.58
IGR J14515−5542	1.0–6.0	5.31	$1.37^{+0.20}_{-0.20}$	$0.39^{+0.18}_{-0.16}$	0.71	42.0/54	1.65
IGR J14552−5133	0.5–6.0	3.37	$1.93^{+0.07}_{-0.07}$	...	0.89	73.1/81	1.17
IGR J15539−6142	0.7–7.0	3.01	1.8 (fixed)	$17.6^{+32.8}_{-13.0}$	0.073	10.6/11	2.13
IGR J16351−5806	1.0–6.0	2.47	$1.61^{+0.75}_{-0.68}$	...	0.031	4.4/5	1.98
IGR J16482−3036	0.5–8.3	1.76	$1.71^{+0.11}_{-0.12}$	$0.13^{+0.5}_{-0.06}$	1.13	80.8/96	3.12
IGR J16558−5203	0.4–8.6	3.04	$1.85^{+0.06}_{-0.04}$	...	1.77	221.0/217	3.39
SWIFT J1656.3−3302	0.7–7.0	2.22	$1.36^{+0.23}_{-0.22}$	$0.17^{+0.15}_{-0.14}$	0.49	50.5/61	2.36
IGR J17488−3253	0.5–7.7	5.30	$1.60^{+0.12}_{-0.10}$	$0.21^{+0.08}_{-0.07}$	1.40	133.1/137	4.03
IGR J18244−5622	2.0–8.0	0.75	$1.94^{+1.86}_{-1.39}$	$14.1^{+15.4}_{-7.9}$	0.67	12.0/13	2.54
IGR J18259−0706	1.0–7.0	7.10	$1.40^{+0.51}_{-0.47}$	$0.62^{+0.40}_{-0.33}$	0.54	13.2/21	1.60
IGR J19443+2117	0.5–8.2	8.28	$1.96^{+0.12}_{-0.11}$	$0.34^{+0.13}_{-0.11}$	1.85	139.0/127	1.93
IGR J20186+4043	1.0–8.0	12.0	1.8 (fixed)	$20.0^{+20.2}_{-12.3}$	0.17	2.8/6	2.24
IGR J20286+2544	1.0–7.0	2.62	1.8 (fixed)	$42.3^{+20.8}_{-19.5}$	2.35	12.4/14	5.64
IGR J21178+5139	1.0–6.2	14.3	1.8 (fixed)	$2.11^{+1.52}_{-1.03}$	0.21	21.4/27	2.26
IGR J21247+5058[b]	1.0–8.5	11.1	$1.44^{+0.12}_{-0.12}$	$1.15^{+0.27}_{-0.25}$	5.20	196.2/175	11.02
SWIFT J2127.4+5654	0.8–7.0	7.87	$1.88^{+0.05}_{-0.05}$	...	2.20	187.2/181	2.71
NGC 7603[b]	0.2–7.5	0.41	$2.05^{+0.03}_{-0.04}$	...	2.40	375.4/231	4.10
SWIFT J0601.9−8636	0.5–5.0	1.10	$1.08^{+2.30}_{-1.08}$	...	0.011	3.5/2	3.23
SWIFT J1009.3−4250	0.3–6.0	1.09	$2.51^{+0.69}_{-0.20}$	$29.5^{+9.60}_{-6.60}$	0.22	12.2/9	2.87
SWIFT J1038.8−4942	0.5–6.8	0.27	$1.11^{+0.13}_{-0.12}$	$0.62^{+0.12}_{-0.10}$	1.45	109.2/108	1.45
SWIFT J1238.9−2720	2.0–7.5	0.67	$1.71^{+0.70}_{-0.60}$	$59.2^{+25.5}_{-20.2}$	0.53	28.5/30	3.92

[a] If the source has a flux variability this is a mean flux.
[b] Source has flux variability.
[c] Source fitted with a model consisting of two power laws (only one intrinsically absorbed) having the same photon index and relative normalization, one being 0.6% of the other; an equally good fit is obtained with the unabsorbed power-law component substituted by a blackbody model with kT $\sim$ 0.2 keV and a luminosity of $\sim10^{41}$ erg s^{-1}
[d] Data allowed only a rough estimate of the flux

infrared) spectroscopy in order to be definitely confirmed as AGNs In the meantime, X-ray spectroscopy can shed light on their extragalactic nature.

3. *Swift* XRT SPECTRAL ANALYSIS

Events for spectral analysis were extracted within a circular region of radius 20′, which encloses about 90% of the point-spread function at 1.5 keV (Moretti et al. 2004) centered on the source position. The background was extracted from various source-free regions close to the X-ray source of interest using both circular/annular regions of various radii, in order to ensure an evenly sampled background. In all cases, the spectra were extracted from the corresponding event files using XSELECT software and binned using GRPPHA so that the χ^2 statistic could reliably be used. We used the latest version (ver. 008) of the response matrices and created individual ancillary response files (ARF) using XRTMKARF. Spectral analyses have been performed using XSPEC version 12.2.1. For those sources with more than one pointing, we performed the spectral analysis of each observation and then of the combined spectra, in order to improve the statistical quality of the data; in most cases spectra from the individual pointings were compatible with each other within the respective uncertainties, thus justifying a combined analysis. Only in five cases (see sources labeled with footnote b in Table 2), do we find evidence for variability between measurements, but always in flux and not in spectral shape; clearly, for these five sources, the reported 2–10 keV flux is an average over a number of observations. Due to the low statistics available, we have identified for each source the best energy range for the spectral analysis and have employed a simple power law absorbed by both a Galactic and an intrinsic column density as our baseline model. The results of the analysis of the combined observations are reported in Table 2, where we list the energy band used for the spectral fit, the Galactic absorption according to Dickey & Lockman (1990), the photon index, the

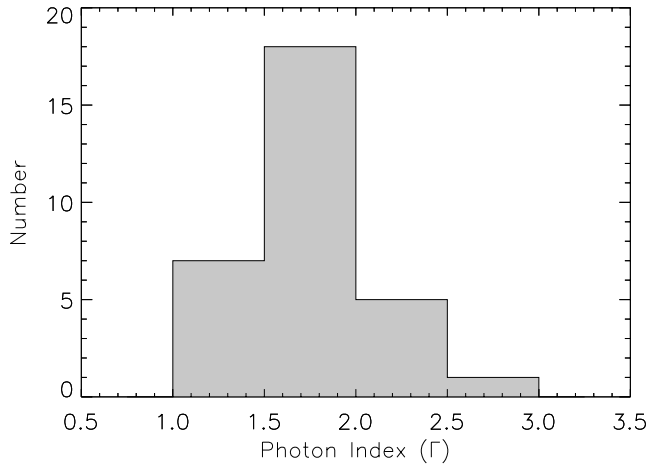

FIG. 1.—Distribution of the photon index of the AGN with optical identifications.

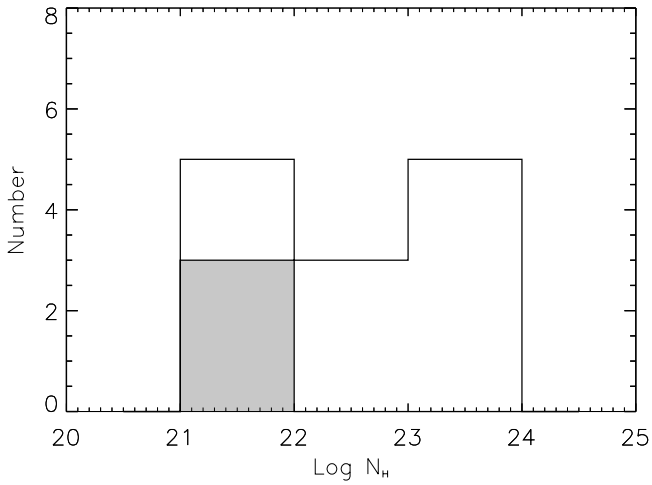

FIG. 3.—Column density distribution of the type 2 Seyferts of our sample, shaded areas are for upper limits.

column density in excess to the Galactic value, if any, the 2–10 keV flux, and the reduced χ^2 of the fit. In the last column of Table 2 we also list the IBIS 20–100 keV flux as reported by Bird et al. (2007). In a few cases the photon index was fixed to the canonical AGN value ($\Gamma = 1.8$), so as to allow a measurement of the intrinsic column density; in the particular case of IGR J14175−4641 only a rough estimate of the 2–10 keV flux was allowed by the data. The presence of the iron line around 6.4 keV, a typical feature of an AGN spectrum, is not statistically required in any of the spectra analyzed, but this is definitely due to the instrument sensitivity and lack of good coverage at these energies. For those sources where there is coverage at low energies (<1 keV), we have checked for the presence of possible soft excess component. In only one case, the Seyfert 1 galaxy ESO 323-G077, do we find significant evidence for this extra component, which could be equally well fitted with an unabsorbed power law having the same photon index of the primary continuum or a blackbody model with $kT \sim 0.2$ keV (see Table 2). All quoted errors correspond to 90% confidence level for a single parameter of interest ($\Delta\chi^2 = 2.71$).

4. PHOTON INDEX AND COLUMN DENSITY DISTRIBUTIONS

Despite the short exposures available, it is still possible to obtain information on the spectral shape of the objects analyzed. In particular, we concentrate here on the photon index distribution and on the absorption properties. To enlarge the sample, we have included four more XRT/IBIS AGNs: SWIFT J0601.9−8636 (Sey 2, $z = 0.006$), SWIFT J1009.3−4250 (Sey 2, $z = 0.033$), SWIFT J1038.8−4942 (Sey 1.5, $z = 0.060$), and SWIFT J1238.9−2720 (Sey 2, $z = 0.024$), already discussed by Landi et al. (2007). Their spectral data have been reanalyzed in the same way as for the other sources presented in this work, and the results are included in the following discussion.

The distribution of photon indices for those AGNs with optical classification is shown in Figure 1; sources where Γ was not constrained by the data were not considered. It is well known that the distribution of X-ray spectral slopes of AGNs peaks around 1.9 and has a nonnegligible dispersion (0.2–0.3; see, e.g., Mateos et al. 2005, and references therein). We obtain a mean Γ value of 1.88 with a dispersion of 0.12, i.e., most of our objects have spectra close to the canonical AGN value. Flat ($\Gamma < 1.5$) spectra are far less common, especially in view of the large uncertainties associated with the XRT spectra; nevertheless, they exist for some sources, such as IGR J21247+5058, as has been confirmed by a recent *XMM-Newton* observation (Molina et al. 2007). The photon index distribution can also be used to characterize unclassified objects: SWIFT J0216.3+5128, IGR J14003−6326, IGR J19443+2117, and possibly IGR J21178+5139 have spectral slopes typical

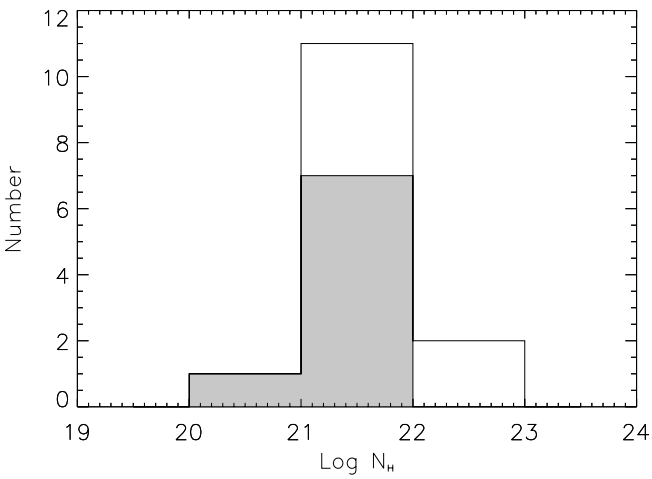

FIG. 2.—Column density distribution of the type 1 Seyferts of our sample, shaded areas are for upper limits.

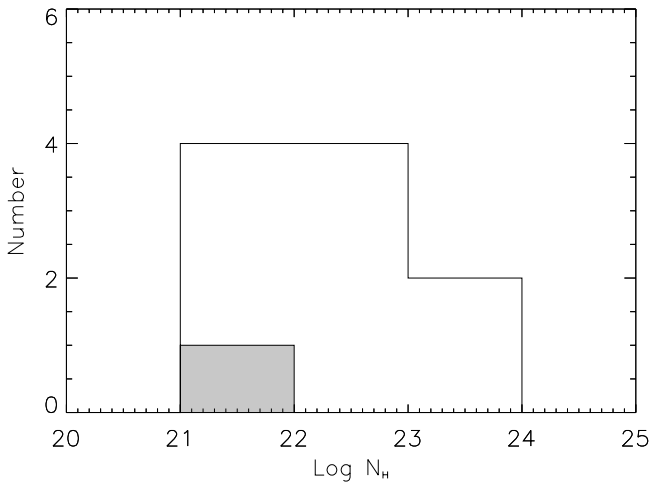

FIG. 4.—Column density distribution of the still unclassified subset of objects, shaded areas are for upper limits.

of AGNs, supporting their extragalactic nature. Others have flat spectra (1.1–1.5) which are unusual, but still compatible with an AGN association.

The column density distribution for each class of objects (type 1, type 2, and unclassified), are shown in Figures 2, 3, and 4, respectively. As we can see from Table 2, various sources of the sample (eight Sey 1s, three Sey 2s, and one unclassified) do not show intrinsic absorption, and therefore their Galactic column density has been taken as an upper limit to the value of $N_{\rm H}$; these sources are reported in the histograms as shaded areas. Absorption in excess of the Galactic value has been measured in 25 objects (around 66% of the sample), but only 16 (47%) have a column density in excess of 10^{22} cm^{-2} (typically taken as the dividing line between absorbed and unabsorbed objects).[8] Absorption was found in 15% of type 1 AGNs, in 73% of type 2 AGNs, and in 60% of unclassified objects. Indeed, the column density distribution of type 1 and type 2 AGNs is significantly different; while type 1 objects cluster in the 10^{21}–10^{22} cm^{-2} range, type 2 sources have a much wider distribution. The distribution of unclassified objects resembles that of Sey 2s, suggesting that many of these sources could be of this type.

5. DISCUSSION

The basic hypothesis of the unified theory of AGNs is that the X-ray absorption and optical obscuration are heavily related; absorbed AGNs should be classified as type 2 in optical (with the broad-line region hidden), while unabsorbed ones are expected to be of type 1 (with the broad-line region visible). This relationship is not always respected, as is evident in our sample, where we find absorption in two Sey 1s (ESO 323-G077 and IGR J21247+5058) and lack of it in a number of Sey 2s. While IGR J21247+5058 is located on the Galactic plane, so that the excess absorption may be due to extra material along the line of sight, ESO 323-G077 is high in Galactic latitude, and so it is likely to be intrinsically absorbed. Evidence of heavily absorption was first reported by Sazonov & Revnivtsev (2004) in the *Rossi X-Ray Timing Explorer* (*RXTE*) survey; also, this AGN is peculiar for being one of the rare cases of a high scattering polarization Sey 1 (Smith et al. 2004). Within the standard model of Seyfert nuclei, both peculiarities of ESO 323-G077 can be well understood by assuming that this AGN is observed at an inclination angle where the nucleus is partially obscured by the torus (hence the high absorption measured in X-rays) and is seen mainly indirectly in the light scattered by dust clouds within or above the torus (hence the high linear polarization observed). Further X-ray observations of this object are clearly desirable because of the constraints that can be derived on the geometric properties of the absorbing region. Contrary to unified models, we have also found five Sey 2s with no clear evidence of absorption in their X-ray spectra. Several authors have reported similar examples of AGNs with no broad emission lines and low $N_{\rm H}$ (Panessa & Bassani 2002; Corral et al. 2005). There are various explanations for this discrepancy, including the low statistical quality of the X-ray spectra and the nonsimultaneity of the optical and X-ray observations. The low X-ray exposures available are clearly the most important source of uncertainty. Alternatively, it is possible that these Sey 2s are either Compton-thick type 2 AGNs or "true" Sey 2s, i.e., objects where the broad-line region is not hidden but likely not to be present. If the source is Compton thick, the 2–10 keV emission is completely blocked and could be seen as reflected/scattered radiation with no apparent absorption. On the other hand, the soft gamma-ray photons are unaffected by absorption as long as $\log N_{\rm H}$ is below 24.5; for higher column densities, even emission above 20 keV is blocked and can only be seen indirectly. Generally, indirect arguments allow discrimination between the Compton-thick and Compton-thin nature of type 2 AGNs, such as the equivalent width of the iron line and the ratio of isotropic versus anisotropic luminosities, typically $L_{\rm X}/L_{[\rm O\ III]}$[9] (Bassani et al. 1999; Panessa & Bassani 2002). Unfortunately, we do not have such information for most of our sources and so we have to rely on a new diagnostic diagram. Figure 5 is a plot of the absorption versus the flux softness ratio ($F_{2-10\ \rm keV}/F_{20-100\ \rm keV}$); a clear trend of a decreasing softness ratio as the absorption increases is visible, as expected if the 2–10 keV flux is progressively depressed as the absorption becomes stronger. Open symbols in the figure represent upper limits on the column density, while lines represent the expected values for an absorbed power law with photon index of 1.5 and 1.9. As anticipated, most of our sources follow the expected trend, except for a few objects which have a too low softness ratio for the observed column density, suggesting a Compton-thick nature. Indeed, if we take the *Swift* XRT observation of Mrk 3, a confirmed Compton-thick Sey 2, and treat it as one of our sources, we find that it is located in the same region, while the true column density of this source is 1.3×10^{24} (Cappi et al. 1999).

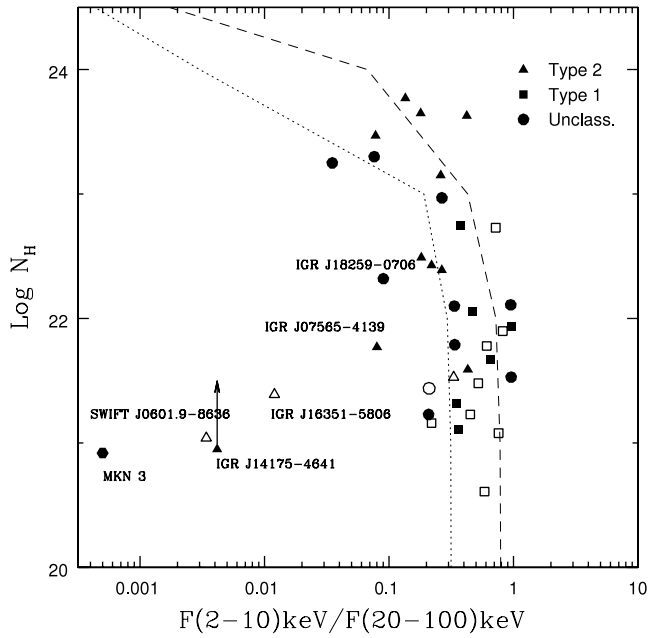

FIG. 5.—$F_{2-10\ \rm keV}/F_{20-100\ \rm keV}$ flux ratio of our enlarged sample. Open symbols represent upper limit values of the column densities and lines correspond to expected values for an absorbed power law with photon index 1.5 (*dotted line*) and 1.9 (*dashed line*). [*See the electronic edition of the Journal for a color version of this figure*.]

We therefore suggest that IGR J14175−4641, IGR J16351−5806, and SWIFT J0601.9−8636 are new Compton-thick AGN candidates where further, more sensitive X-ray observations, particularly around the iron line, could help in confirming these results. Similarly, IGR J07565−4139 and IGR J18259−0706 are outside the expected trend, although their softness ratio is not so dramatically low and could be explained by the uncertainties associated with the flux estimates as well as by variability in the source, since the X-ray and soft gamma-ray fluxes are not taken simultaneously. While for IGR J18259−0706 we must await the

[8] This $N_{\rm H}$ value represents the amount of absorbing neutral gas needed to hide the broad emission-line region (BLR), assuming a Milky Way gas-to-dust ratio.

[9] The $L_{[\rm O\ III]}$ is corrected for reddening in the host galaxy by means of the Hα/Hβ Balmer decrement.

source classification to confirm its extragalactic nature and therefore the presence of any peculiarity, IGR J07565−4139 is intriguing, as the soft X-ray emission is unlike any other seen in a small sample of absorbed AGNs (De Rosa et al. 2007). Two more unabsorbed Sey 2s, IGR J12415−5750 and IGR J14515−5542, are also anomalous but are unlikely to be Compton-thick objects, as their location is well within the expected region of $N_{\rm H}$ versus $F_{2-10\,\rm keV}/F_{20-100\,\rm keV}$; while IGR J12415−5750 may have been misclassified in optical,[10] IGR J14515−5542 shows a true Sey 2 spectrum and, furthermore, has a $L_{\rm X}/L_{[\rm O\,III]}$ ratio typical of unabsorbed type 1 sources (Masetti et al. 2006c), and so it qualifies as a "true" Sey 2 nucleus; indeed, the observed column density barely explains the occultation of its broad-line region.

6. CONCLUSIONS

Swift XRT follow-up X-ray observations of 34 *INTEGRAL* IBIS AGNs and AGN candidates have pinpointed their X-ray counterparts, allowing the unambiguous identification of the soft gamma-ray source and the determination of the AGN class, in most cases. Furthermore, for most objects in the sample, the photon index and absorption have been measured. When this sample is enlarged to include four more AGNs already discussed in the literature, we find a mean photon index of 1.88, with a dispersion of 0.12. Of the objects, 47% have column densities in excess of 10^{22} cm^{-2}, and, as expected, a large fraction of the absorbed sources are within the Sey 2 sample. We have provided a new diagnostic tool ($N_{\rm H}$ vs. $F_{2-10\,\rm keV}/F_{20-100\,\rm keV}$ softness ratio) with which to isolate or find a few peculiar objects: (1) two absorbed Sey 1 galaxies (ESO 323-G077 and IGR J21247+5058); (2) three Compton-thick AGN candidates (SWIFT J0601.98636, IGR J14175−4841, and IGR J16351−5806); and (3) at least one secure example (IGR J14415−5542) of a "true" type 2 AGN, i.e., one where the broad-line region is not hidden but likely not to be present. Within the sample of 10 still unidentified objects, 3 (IGR J14492−5535, IGR J15539−6142, and IGR J20186+4043) are almost certainly AGNs of type 2; 3–4 more (SWIFT J0216.3+5128, IGR J14003−6326, IGR J19443+2117, and possibly IGR J21178+5139) have spectral slopes typical of AGNs (with the first two likely to be of type 2 because of the measured absorption). Two objects (IGR J13109−5552 and SWIFT J16563−3302) are located high enough off the Galactic plane and are strong radio emitters and are therefore good AGN candidates; only IGR J18259−0706 has a doubtful AGN association, despite being a radio source.

[10] See http://www.astro.umd.edu/∼lwinter/research/BAT/xray.html.

We acknowledge the Italian Space Agency financial and programmatic support via contracts I/R/046/04 and I/023/05/0. A. M. thanks J. B. Stephen for a careful reading of the manuscript.

REFERENCES

Barthelmy, S. D., et al. 2005, Space Sci. Rev., 120, 143
Bassani, L., et al. 1999, ApJS, 121, 473
Bird, A. J., et al. 2007, ApJS, 170, 175
Burrows, D. N., et al. 2005, Space Sci. Rev., 120, 165
Cappi, M., et al. 1999, A&A, 344, 857
Corral, A, Barsons, X, Carrera, F. J., Ceballos, M. T., & Mateos, S. 2005, A&A, 431, 97
De Rosa, A., et al. 2007, A&A, submitted
Dickey, J. M., & Lockman, F. J. 1990, ARA&A, 28, 215
Gehrels, N., et al. 2004, ApJ, 611, 1005
Halpern, J. P. 2006, ATel, 847
Hill, J. E., et al. 2004, Proc. SPIE, 5165, 217
Landi, R., et al. 2007, ApJ, in press
Masetti, N., et al. 2006a, A&A, 449, 1139
Masetti, N., et al. 2006b, A&A, 455, 11
———. 2006c, A&A, 459, 21
Mateos, S., et al. 2005, A&A, 444, 79
Molina, M. 2004, Laurea thesis, Bologna Univ.
Molina, M., et al. 2007, MNRAS, submitted
Moretti, A., et al. 2004, Proc. SPIE, 5165, 232
Panessa, F., & Bassani, L. 2002, A&A, 394, 435
Sazonov, S., & Revnivtsev, M. G. 2004, A&A, 423, 469
Sazonov, S., Revnivtsev, M. G., Krivonov, R., Churazov, E., & Sunyaev, R. 2007, A&A, 462, 57
Smith, J. E., et al. 2004, MNRAS, 350, 140
Ubertini, P., et al. 2003, A&A, 411, L131
Winkler, C., et al. 2003, A&A, 411, L1